Reconstruction of Pristine and Hydrolyzed Quartz Surfaces

Vladimir V. Murashov[†]

National Institute for Occupational Safety and Health, Morgantown, West Virginia

Received: March 10, 2004

Reconstruction of the most common pristine and hydrolyzed surfaces of quartz was investigated with periodic density functional theory calculations. Surface energies of reconstructed pristine faces, pertinent to quartz growth morphologies in melts, are found to range from 0.071 eV/Å^2 for the (101) surface to 0.139 eV/Å^2 for the (001) surface, and they increase as (101) < (102) < (112) < [(100), (111)] < (110) < (001). Four types of reconstruction reactions are observed: (1) formation of two-membered rings from vicinal silyl and siloxy sites, (2) formation of a pair of tricoordinated/unicoordinated oxygen atoms, (3) formation of three-membered rings, and (4) transformation of silanone sites into siloxane sites. The main features of reconstructed pristine quartz surfaces are two-membered rings formed from bridged siloxy and silyl sites on all investigated surfaces, a stable site complex with geminal positively charged tricoordinated and negatively charged unicoordinated oxygen atoms revealed on the (112) surface, and charged nonbridged siloxy/silyl sites, which are more stable than radical siloxy/silyl sites. Hydrolyzed surface energies range from −0.010 eV/Å^2 for the (001) surface to 0.002 eV/Å^2 for the (101) surface and increase as (001) < (110) < (102) < (111) < (100) < (112) < (101). The hydrolyzed surface stability is found to depend strongly on inter-site silanol hydrogen bonding. Observed networks of hydrogen bonds are important for interactions between silica surfaces and biomolecules in an aqueous environment.

Introduction

Silica or silicon dioxide is a ubiquitous chemical compound most commonly found in a form of quartz. Being a major constituent of rocks, it composes a significant part of rock dust produced in mining, construction, and various manufacturing processes. Inhaled quartz dust causes an increased risk of pulmonary fibrosis, pneumoconiosis, silicosis, and cancer.[1] The toxicity of crystalline silica polymorphs has been a topic of intense research for many decades. Still, the mechanism of silica toxicity remains elusive. One of the widely accepted hypotheses attributes the toxicity of crystalline silica to interactions between silica surface sites and biomolecules.[2] Specifically, adsorption of biomolecules on geminal silanol groups was proposed as a possible mechanism of silica toxicity.[3] Knowledge of the atomic structure of silica surfaces is also crucial for progress in semiconductor technology, synthesis of silica-based functional materials, sorption, and catalysis.

There have been only limited experimental ESR, IR, and optical absorption spectroscopy data on silica surface sites.[4] Surface silyl and siloxy radicals have been studied with ESR measurements.[5] Calculations of silanone and siladioxirane sites have been performed to help in identifying bands on photoabsorption[6] and photoluminescence[7] spectra of silica and oxidized silicon surfaces. Silanone sites have been detected with IR spectroscopy on surfaces of mechanically treated silica.[8] Formation of two-membered silicon rings[9] upon thermal treatment under vacuum above 720 K was used to explain a pair of strong IR bands at 908 and 888 cm^{-1}.[10] This structure hydrolyzes in the presence of water with formation of two single silanol groups.[11] ^{29}Si NMR can be used to quantitatively determine the ratio of geminal and single/isolated silanol groups.[12] X-ray photoelectron spectroscopy (XPS) can also be used to characterize the degree of polymerization of silica surface sites.[13] Thus, an experimental XPS study of polished polycrystalline quartz found that the atomic ratio between surface oxygen atoms and surface silicon atoms was 1.8, thus suggesting that most of the surface silanol sites are geminal.[14] Natural bonding orbital (NBO) analysis of silica clusters was used to characterize bonding in silica surface sites.[15]

To date, there have been a few reports investigating a limited number of reconstructed[16] quartz surfaces. An experimental low-energy electron diffraction (LEED) study of the (001),[17] (100), and (101)[18] surfaces showed the presence of (1 × 1) patterns on pristine quartz surfaces. This reconstruction of the (001) surface also agrees with periodic density functional theory (DFT) calculations,[19] which suggested the possibility of a high-density (1 × 1) reconstruction after annealing at 300 K. Previous studies[20] revealed that unrelaxed surface energies of correlated low-index crystal forms of quartz differ by less than 0.003 eV/Å^2 or 2%. It was also shown that different site configurations for a given unrelaxed surface can differ by as much as 0.036 eV/Å^2 (Q^2(:)/Q^2(O)$_2$ and Q^2(O)/Q^2(O)[21] configuration on the {001} correlated form) or by 19%. An experimental X-ray reflectivity and atomic force microscopy study[22] of the quartz (100)− and (101)−water interfaces showed that most of the surface silanol groups are single with only some geminal silanediol groups found on the (100) surface. Vertical reconstruction of the silica surface layer was found to be limited to a depth of 14 Å. Periodic DFT calculations of the hydroxylated (011) and (001) surfaces[23] and atomistic calculations of the hydroxylated (001), (100), (101), (10$\bar{1}$)[24] and (011) surfaces[25] showed the presence of intersite silanol hydrogen bonds.

In this work, reconstruction of pristine and hydrolyzed low-index quartz surfaces, (101), (102), (112), (100), (111), (110), and (001), which were found in an earlier study[20] to be low-energy correlated forms with low-energy unreconstructed site configurations, has been investigated and hydrogen-bond net-

[†] Current address: National Institute for Occupational Safety and Health, 200 Independence Ave. SW, Room 733"G", Washington, DC 20201. E-mail: vem8@cdc.gov.

10.1021/jp0402075 CCC: $30.25
Published on Web 02/08/2005

works of single silanol, ≡Si(OH), and silanediol, =Si(OH)$_2$, groups have been characterized using periodic DFT computational techniques in order to facilitate the understanding of mechanisms of adsorption and chemical reactions of biomolecules on silica surfaces. This work is another step in an ongoing research program directed toward delineating mechanisms of silica pathogenicity.

Computational Methods

All DFT periodic calculations were performed with the VASP simulation package.[26,27] The gradient-corrected exchange correlation functional of Perdew-Wang[28] was used. Electronic wave functions were modeled with the plane-wave basis set using the projector-augmented wave (PAW) method[29] applied to ultrasoft Vanderbilt-type pseudopotentials[30] produced by the Institut für Theoretische Physik, TU Wien.[31] The energy cutoff for the plane wave basis set was fixed at 500 eV. The Brillouin zone was sampled with the Monkhorst−Pack technique[32] using $3 \times 3 \times 1$ k-points mesh. Integration was performed using the tetrahedron method[33] with Blöchl corrections.[34] Relaxation of ions into a minimum-energy state was performed with a conjugate gradient algorithm. Atoms of surface silica tetrahedra, with altered internal and external bonding, were allowed to move (either in energy optimization routines or in molecular dynamics calculations). The optimization was terminated when the estimated error in the total energy was less than 10^{-4} eV for both the electronic and ionic minimizations. Initially, the minimum energy density of bulk quartz was located by a set of energy minimization calculations on orthogonal cells of the optically right-handed α-quartz[35] with fixed volumes. To change the cell volume, unit cell parameters were scaled, while directional cosines were kept fixed. The resulting unit cell parameters were 3% larger than those experimentally observed for quartz under ambient conditions.[36] Thus, the cell was characterized by the following unit cell parameters: $a = 5.057$ Å (4.910 Å),[37] $c = 5.564$ Å (5.402 Å). The optimized quartz structure has SiOSi angles of 149.9° (143.0°), SiOSiO pairs of torsion angles of 46.2/115.8° (31.1/131.4°) and −3.4/−73.6° (15.8/−93.3°), half of the Si−O bond lengths at 1.625 Å (1.600 Å) and the other half at 1.627 Å (1.615 Å). A structure optimized in this way was used to prepare slabs with surfaces of the (101), (102), (112), (100), (111), (110), and (001) indices separated by a vacuum layer of 10 Å.[38] Parameters of supercells containing slabs separated by vacuum are given in Table 1. Initial configurations of hydrolyzed surfaces were created by saturating broken bonds with hydroxyls or hydrogen atoms to obtain fully hydroxylated surfaces. Initial vacuum separation between unreconstructed pristine surfaces of slabs used to prepare hydrolyzed surfaces was set to 15 Å. The resulting supercells composed of crystal slab/vacuum sandwiches were subjected to periodic boundary conditions. Stabilities of optimized geometries were confirmed by molecular dynamics NVT calculations at $T = 300$ K for 1000 steps with a time step of 1 fs followed by structural minimization.

Energies of the water molecule and water dimer were calculated in a cubic cell with 10 Å side length. The Brillouin-zone sampling was restricted to the Γ point. The Gaussian smearing method with the width of smearing set to 0.3 was used to facilitate calculation of accurate band-structure energy. Calculated total energy values extrapolated to the zero width of smearing are $E_{H_2O} = -14.2735$ eV for the monomer and $E_{2H_2O} = -28.7653$ eV for the dimer. Thus, the energy of a single hydrogen bond can be estimated at $E_{Hb} = -0.2184$ eV or −21.1 kJ/mol. This value is very close to the experimental one of −23.0 kJ/mol.[39]

TABLE 1: Dimensions of Supercells, the Number of Mobile Atoms, and the Number of Molecular Units (n for SiO_2, m for H_2O) in Supercells Used in Periodic DFT Calculations of Pristine and Hydrolyzed Surfaces

				supercell dimensions					
surface	type	no. of relaxing atoms	$n//n+m$	a(Å)	b(Å)	c(Å)	α(deg)	β(deg)	γ(deg)
(101)	pristine	16	12	7.519	5.057	22.956	90	90	109.65
	hydrol	22	12 + 2	7.519	5.057	29.576	90	90	109.65
(112)	pristine	30	18	8.760	7.519	20.448	90	90	90
	hydrol	42	18 + 4	8.760	7.519	28.099	90	90	90
(100)	pristine	11	12	5.057	5.564	27.202	90	90	90
	hydrol	17	12 + 2	5.057	5.564	32.836	90	90	90
$(100)^S$	pristine	14	11	5.057	5.564	26.765	90	90	90
	hydrol	20	11 + 2	5.057	5.564	31.765	90	90	90
$(100)^G$	pristine	8	10	5.057	5.564	26.765	90	90	90
	hydrol	14	10 + 2	5.057	5.564	31.765	90	90	90
(111)	pristine	22	12	7.519	7.519	20.610	90	90	108.75
	hydrol	34	12 + 4	7.519	7.519	24.554	90	90	108.75
(001)	pristine	16	12	10.115	5.057	20.807	90	90	120
	hydrol	28	12 + 4	10.115	5.057	26.449	90	90	120
(110)	pristine	19	12	5.564	8.760	20.788	90	90	90
	hydrol	31	12 + 4	5.564	8.760	25.788	90	90	90
(102)	pristine	22	12	10.377	5.057	19.393	90	90	90
	hydrol	34	12 + 4	10.377	5.057	25.114	90	90	90

The energy of a pristine surface was calculated as $E_{surf} = (E_{slab} - nE_{bulk})/S$, where E_{slab} is energy of a pristine slab, $E_{bulk} = -23.8883$ eV per SiO_2 molecule, $n = 12$ is the number of SiO_2 molecules in a supercell (due to a high surface area and a large number of exposed silica tetrahedra resulting in a high number of relaxed atoms in the simulation supercell; $n = 18$ for the (112) surface), and S is the total surface area formed as a result of cleavage. For hydrolyzed surfaces $E_{surf(OH)} = (E_{slab(mH_2O)} - nE_{bulk} - mE_{H_2O})/S$, where $E_{slab(mH_2O)}$ is the energy of a hydrolyzed slab, and m is the number of water molecules required to fully hydrolyze both complementary surfaces of the slab. The surface energy without hydrogen bond energy is approximated as $E_{surf-Hb} = (E_{slab(mH_2O)} - nE_{bulk} - mE_{H_2O} - kE_{Hb})/S$, where k is the number of hydrogen bonds shorter than 2.0 Å. The energy of hydroxylation was estimated as $E_{hydr} = 96.48(E_{slab(mH_2O)} - E_{slab(relx)} - mE_{H_2O})/m$, where $E_{slab(relx)}$ is the energy of a slab with reconstructed pristine surfaces in eV and 96.48 kJ/(eV mol) is a conversion factor to obtain results in kJ/mol.

Since complementary surfaces obtained by crystal cleavage are different in general, calculated surface energies reported in Tables 2 and 3 incorporate both complementary surfaces. Complementary surfaces are represented by the opposing sides of model slabs. They are distinguished by the following notation: data pertaining to the side of a slab located in the center of the modeling cell are distinguished by the letter U (side facing up) and data referring to the other side of the slab are distinguished by the letter D (side facing down). Complementary surfaces resulting from cleavage along the (100) surface are covered exclusively by either silanone Q^2(O) sites (side D) or Q^3 sites (side U). To estimate the relative stability of these complementary cleavage faces, (100) slabs with both sides covered with either of the sites are also considered. Thus, the $(100)^S$ slab has both sides covered with Q^3 sites (after hydrolysis these sites become single silanol groups, hence the superscript S) and the $(100)^G$ slab is covered with Q^2(O) sites (after hydrolysis these sites become geminal silanediol groups, hence the superscript G).

Results and Discussion

Geometry of Reconstructed Quartz Surface Sites. Cleavage of silica can proceed via two main mechanisms: homolytic and heterolytic. In the former, a pair of electrons of a ruptured

TABLE 2: Calculated Energies of Pristine Quartz Surfaces

	unreconst compl surfaces			reconst compl surfaces			
surface	sites U/D	$-E_{slab}$ (eV)	E_{surf} (eV/Å^2)	sites U/D	$-E_{slab(relx)}$ (eV)	$E_{surf(relx)}$ (eV/Å^2)	$-E_{rec}$ (eV/Å^2)
(101)	$Q^3(O^-) + Q^3(+)/Q^3(O^-)+Q^3(+)$	275.0290	0.162	R^2/R^2	281.5989	0.071	0.091
(112)	$2[Q^3(O^-) + Q^3(+)]/2[Q^3(O^-) + Q^3(+)]$	406.1261	0.181	$R^2 + Q^3(O^-) + Q^3(+)/R_2^2(+) + Q^3(O^-)$	415.6773	0.109	0.072
(100)	$Q^3(O^-) + Q^3(+)/Q^2(O)$	276.7203	0.177	$R^2/Q^2(O)$	280.4860	0.110	0.067
(100)^S	$Q^3(O^-) + Q^3(+)/Q^3(O^-) + Q^3(+)$	251.7238	0.196	R^2/R^2	256.3850[a]	0.113	0.083
					256.9392[b]	0.104	0.092
(100)^G	$Q^2(O)/Q^2(O)$	229.8201	0.161	$Q^2(O)/Q^2(O)$	232.2892	0.117	0.044
(111)	$Q^2(O) + Q^3(O^-) + Q^3(+)/Q^2(O) + Q^3(O^-) + Q^3(+)$	265.9823	0.193	$Q^2(O) + R^2/Q^2(O) + R^2$	274.8508	0.110	0.083
(001)	$2Q^2(O)/2Q^2(O)$	269.5600	0.193	$2Q^2(O)/2Q^2(O)$	274.3063	0.139	0.054
(110)[c]	$2Q^2(O)/Q^2(O) + Q^3(O^-) + Q^3(+)$	267.4595	0.197	$2Q^2(O)/Q^3(O^-)+Q^3(+)$	273.9296	0.131	0.066
(110)[d]	$2Q^2(O)/Q^2(O) + Q^3(O\bullet) + Q^3(\bullet)$	267.3513	0.198	$2Q^2(O)/Q^3(O\bullet)+Q^3(\bullet)$	272.8522	0.142	0.056
(102)	$Q^2(O) + Q^3(+) + Q^3(O^-)/Q^2(O) + Q^3(O^-) + Q^3(+)$	265.3147	0.203	$Q^2(O) + R^2/Q^2(O) + R^2$	275.4544	0.107	0.096

[a] R^2 on 6-fold helices. [b] R^2 on 3-fold helices. [c] Spin-paired calculations. [d] Spin-polarized calculations with $N_\alpha - N_\beta = 2$.

TABLE 3: Calculated Energies of Hydrolyzed Quartz Surfaces in Periodic Calculations and the Number of Hydrogen Bonds Shorter than 2.00 Å (k)[a]

surface	silanols U/D	k U/D	$-E_{slab(mH_2O)}$ (eV)	$E_{surf(OH)}$ (eV/Å^2)	$E_{surf-Hb}$ (eV/Å^2)	$-E_{hydr}$ (kJ/mol) (H_2O)
(110)	2G/2S + 1G	0/2	344.3974	−0.007	−0.002	323
(102)	2S + 1G/2S + 1G	1/1	344.2580	−0.005	−0.001	282
(111)	2S + 1G/2S + 1G	1/1	344.2065	−0.004	0.000	296
(100)	2S/1G	1/0	315.3726	−0.003	0.001	306
(100)^S	2S/2S	1/1	291.6738	−0.006	0.001	298
(100)^G	1G/1G	0/0	267.3835	0.001	0.001	316
(112)	4S/4S	0/0	486.9372	0.001	0.001	342
(101)	2S/2S	0/0	315.0902	0.002	0.002	239
(001)	2G/2G	4/4	344.6731	−0.010	0.009	320

[a] The number of silanol groups in a supercell is given in front of the silanol type: S, single silanol; G, silanediol.

chemical bond is divided evenly between Si and O atoms forming two radicals, such as silyl $Q^3(\bullet)$ and siloxy $Q^3(O\bullet)$, while in the latter case the pair of electrons gets transferred to a more electronegative atom (oxygen in this case), forming charged species. There could be one, two, or three bonds broken per surface silicon atom, leading to Q^3, Q^2, and Q^1 sites, respectively. If there are two broken bonds per surface silicon atom (Q^2 sites), it is possible to further divide the classification of homolytic cleavage into symmetric cleavage, leading to each surface silicon doubly bonded to one surface oxygen atom (silanone $Q^2(O)$ sites) and asymmetric cleavage with one of the two surfaces exposing silicon atoms in the formal oxidation state +2 with a lone pair of electrons (silylene $Q^2(:)$ sites) and with the other surface covered with siladioxirane (SDO) $Q^2(O)_2$ sites. Surface reconstruction, which is completed within 2 ps as shown by earlier computer simulations,[40] can lead to the formation of two-membered silicon rings R^2, [−O−Si(<)−O−Si(<)−], from silyl and siloxy sites.[41] These rings can be also viewed as edge-sharing silica tetrahedra.

Earlier computational studies (see for example ref 19) indicated that relaxation of the silica surface layer can extend as deep as six SiO_2 molecular layers. In this study surface relaxation was limited, due to computational limitations, to a single silica-tetrahedral layer only. Residual forces acting on frozen atoms of the slab core imitating restrictions imposed by the "bulk crystal" can be significant, and therefore, some caution should be exercised in interpreting results presented in this work. For example, the (001) slab calculations revealed that forces acting on silicon atoms next to the relaxed SiO_2 surface layer can be as high as 0.27 eV/Å (directed toward the surface), while those acting on oxygen atoms reach 0.35 eV/Å (pointing away from the surface). For testing purposes, an additional four silicon atoms and eight oxygen atoms nearest to the surface were allowed to relax; thus, only four silicon atoms and four oxygen atoms remained frozen in the (001) slab. The resulting (001) relaxed surface lowered its energy by 0.0003 eV/Å^2 or only 0.2%, leaving the value of the surface energy reported in Table 2 unchanged. Bonding patterns around (001) surface sites did not change as a result of the additional relaxation.

Optimized geometries of silica surface sites, obtained in these periodic DFT calculations, correlate very well with those found in cluster calculations:[15] silanone >Si═O bond lengths range from 1.521 Å found on the (111) and (110) surfaces to 1.527 Å found on the (001) surface compared to r_{clust}(>Si═O) = 1.526 Å obtained in cluster calculations; siloxy anion Si−O$^-$ bond lengths range from 1.537 Å for a siloxy anion site geminal to a two-membered silicon ring on the (112) surface to 1.543 Å for the (110) surface compared to r_{clust}(Si−O$^-$) = 1.548 Å; average silyl cation O−Si$^+$ bond lengths range from 1.592 Å for the (112) surface to 1.594 Å for the (110) surface compared to r_{clust}(O−Si$^+$) = 1.576 Å. The cationic silyl site is flat, with the average torsion angle OSiOO for atoms of the site ranging from 174° for the (112) surface to 177° for the (110) surface compared to 179° observed in cluster calculations.[42] A lower planarity of these sites in periodic calculations can be related to geometrical constraints imposed by bulk and surface atoms. Silicon−oxygen bond lengths of radical silica sites are longer than siloxane bond lengths in fully coordinated closed-shell sites, 1.626 Å, which is in agreement with cluster calculations. The siloxy radical Si−O$^\bullet$ bond length on the (110) surface is 1.646 Å compared to r_{clust}(Si−O$^\bullet$) = 1.674 Å, and the average silyl radical O−Si$^\bullet$ bond length is 1.678 Å compared to r_{clust}(O−Si$^\bullet$) = 1.649 Å.[15] Torsion OSiOO angles around the silyl site characterizing the flatness of the site range from 122 to 127° in periodic calculations and from 120 to 125° in cluster calculations.

In two-membered R^2 rings, the Si−O bonds are elongated compared to the bulk Si−O bonds and range from 1.646 to 1.711 Å. Siloxane angles in R^2 rings are strained and range from 90 to 93°. The flatness of the rings, which is characterized by an angle between two normals to the surfaces formed by the Si$^\bullet$···Si ring diagonal and oxygen atoms of the ring, ranges from 5 to 11°. The size of the rings can be characterized by the ring diagonal Si···Si, which ranges from 2.383 to 2.443 Å.

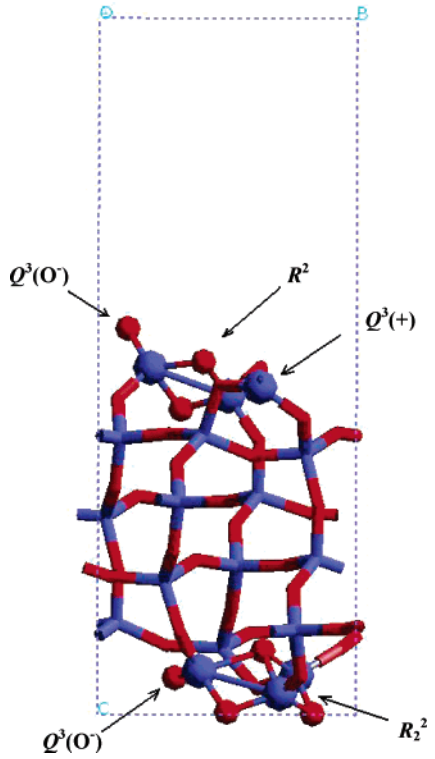

Figure 1. Side projection of a reconstructed slab with pristine (112) complementary surfaces. Atoms of surface sites are shown as spheres: red for oxygen and blue for silicon. Side U of the slab is in the center of the rectangular supercell, and side D is at the bottom of the supercell.

Bond lengths around a tricoordinated oxygen atom of the R_2^2-(+) structure on side D of the reconstructed (112) surface (Figure 1) are 1.997, 1.809, and 1.722 Å. Siloxane bonds in R^2 geminal to the siloxy anion bond are elongated: on the (112) surface they range from 1.781 to 1.997 Å. Accordingly, Si···Si ring diagonals are also elongated and range from 2.406 to 3.581 Å.

The recombination of silyl and siloxy sites with formation of R^2 rings is accompanied by large atomic displacements of up to 2.817 Å for the oxygen atom and 0.942 Å for the silicon atom observed on the (100) surface (Table 4). A silicon atom on side D of the (110) surface, which increases its coordination number from 3 to 4, undergoes the largest shift of 2.357 Å. The second largest displacement for a silicon atom of 1.863 Å is found in a silyl site of a three-membered silicon ring on side U of the (112) slab.

Energy of Reconstruction of Pristine Quartz Surfaces. Unreconstructed surface energies were shown to correlate via Boltzmann statistics with frequency of occurrence of cleaved surfaces obtained by comminution processes.[20] Reconstructed surface energies determine the crystal habits of crystals grown from melts close to equilibrium conditions, while energies of reconstructed hydrolyzed surfaces are pertinent to the distribution of crystal forms among crystals grown from aqueous solutions close to equilibrium conditions.[43]

All investigated surfaces with bridged silyl and siloxy sites undergo reconstruction with the formation of R^2 two-membered silicon rings. The barrier for the $Q^3(O^-) + Q^3(+) \rightarrow$ transformation is found to be high enough to prevent ring formation after annealing at 300 K. The lowest reconstructed surface energy of 0.071 eV/Å^2 is observed in cleavage along the (101) surface, where the lowest concentration of surface two-membered silicon rings is present. The (102), (111), (112), and (100) surfaces have higher reconstructed surface energies of ca. 0.11 eV/Å^2. A complementary (100)^S surface can have R^2 rings formed on 3-fold helical channels or on 6-fold helical channels. The former is lower in energy by 27 kJ/mol. The energy of two-membered-ring formation varies from −226 kJ/mol for the (100)^S surface with R^2 rings formed on 6-fold helical channels to −314 kJ/mol for the (101) surface.

TABLE 4: Maximum Displacements of Surface Atoms in Å

surface		pristine		hydrolyzed	
		Δ(Si)	Δ(O)	Δ(Si)	Δ(O)
(101)	U	0.671	2.030	0.018	0.119
	D	0.668	2.026	0.017	0.124
(112)	U	1.863	1.607	0.026	0.089
	D	1.791	2.466	0.058	0.123
(100)	U	0.936	2.817	0.056	0.227
	D	0.527	0.205	0.045	0.278
(100)^S	U	0.942	2.291	0.084	0.238
	D	0.937	2.293	0.073	0.207
(100)^G	U	0.503	0.231	0.082	0.192
	D	0.503	0.233	0.126	0.295
(111)	U	0.677	2.240	0.154	0.333
	D	0.638	2.054	0.140	0.453
(001)	U	0.742	0.565	0.063	0.301
	D	0.748	0.575	0.073	0.327
(110)^a	U	0.702	0.413	0.147	0.485
	D	2.300	2.561	0.092	0.196
(110)^b	U	0.708	0.406		
	D	2.357	2.582		
(102)	U	0.730	1.968	0.146	0.409
	D	0.803	1.963	0.158	0.437

[a] Spin-paired calculations. [b] Spin-polarized calculations with $N_\alpha - N_\beta = 2$.

Two potential energy minima, which differ in site distribution on side D of the (112) surface, are found: the high-energy zero-order minimum $R^2 + Q^3(O^-) + Q^3(+)$ with surface energy of 0.116 eV/Å^2 and the low energy zero-order minimum $R_2^2(+) + Q^3(O^-)$ with surface energy of 0.109 eV/Å^2. The $R_2^2(+)$ structure has two adjoining two-membered silicon rings with a shared tricoordinated oxygen atom (such a coordination is also observed in stishovite, a high-density crystalline silica polymorph) bearing a formal charge of +1 (Figure 1). One of the oxygen atoms geminal to the tricoordinated oxygen atom is unicoordinated and has a formal charge of −1. Such an alternation of the coordination and charge of oxygen atoms was described earlier as an intrinsic defect in amorphous SiO_2[44] and as a possible product of reconstruction of the (001) quartz surface.[19] On the (112) surface the anionic/cationic pair of geminal oxygen atoms is more stable than the $R^2 + Q^3(+)$ pair by 90 kJ/mol according to our calculations. On side U of the (112) slab the reconstruction $Q^4 + Q^3(O^-) \rightarrow Q^3(O^-) + Q^4$ around a $Q^3(+)$ silyl site takes place, resulting in the formation of a three-membered silicon ring, R^3, containing the silyl site.

An oxygen atom of an originally $Q^2(O)$ site on side D of the (110) surface bridges a silicon atom of a $Q^3(+/\bullet)$ site and one of the siloxane oxygens of the $Q^3(+/\bullet)$ site reconnects to the silicon atom of the $Q^2(O)$ site. The resulting reconstruction reaction can be summed up as $Q^2(O) + Q^3(+/\bullet) \rightarrow Q^4 + Q^3(+/\bullet)$. It also leads to the formation of a four-membered silicon ring, R^4. The (110) surface with charged cationic silyl and anionic siloxy sites has the second highest reconstructed surface energy of 0.131 eV/Å^2. The stability of relaxed radical silyl and siloxy sites on this surface has also been investigated. The relaxed (110) slab in spin-polarized calculations with the number of α-spin electrons higher by two per silyl/siloxy pair ($N_\alpha - N_\beta = 2$) than the number of β-spin electrons is characterized by an average surface energy (by 0.011 eV/Å^2) higher than the energy of the reconstructed slab obtained in paired-electron

calculations with charged silyl/siloxy sites. This corresponds to an energy increase of 104 kJ per mole of silyl/siloxy sites. Cluster calculations suggest that the homolytic cleavage of a single Si−O bond is more favorable energetically than the heterolytic cleavage. For instance, in calculations of silica dimer, the energy of the homolytic cleavage is lower than the energy of the heterolytic cleavage by 332 kJ/mol.[15] This stabilization of surfaces with charged sites could be in part due to favorable intersite electrostatic interactions, which are not incorporated in cluster calculations.

Relaxation of the silanone Q^2(O) site is less drastic than that of other silica surface sites, due to the absence of change in the coordination numbers of surface atoms. It is revealed by a lower relaxation energy and smaller atomic displacements (vide infra). The energy of the Q^2(O) site relaxation ranges from −115 kJ/mol for the (001) surface to −119 kJ/mol for the $(100)^G$ surface. Hence, despite a higher stability of the unreconstructed $(100)^G$ surface with Q^2(O) sites compared to $(100)^S$ surface with Q^3 sites by 95 kJ/mol, after reconstruction the latter is more stable by 35 kJ per mole of Q^2(O) or R^2 sites. This finding suggests that, for the same concentration of broken siloxane Si−O bonds, surfaces with geminal silanediol groups can be more readily formed in mechanical comminution processes in vacuo than those with single silanol groups. On the other hand, the latter can be more prominent on crystals naturally grown from melts or on crystals, which underwent an extensive long-term reconstruction. An experimental X-ray reflectivity study[22] showed that most of the silica groups on the (100) growth surface of their samples are single silanol groups.

A low degree of relaxation of silanone sites and their high concentration on the (001) surface lead to the highest reconstructed surface energy of 0.139 eV/Å^2. Cleavage along this quartz surface can also result in the formation of siladioxirane and silylene sites, which were described earlier.[19,20] Relaxation amounts to 0.029 eV/Å^2, and the relaxed surface energy is 0.200 eV/Å^2 in these calculations. Both relaxed and unrelaxed surface energies in this case are higher than the respective energies of the (001) surface with silanone sites. These calculations revealed only a 1 × 1 reconstruction on the (001) surface. A possible 2 × 1 reconstruction reported in an earlier study[19] was not observed, even after the slab was annealed at 2000 K for 1.5 ps. It could be related in part to limiting reconstruction to a depth of one silica tetrahedron employed in this study.

The order of reconstructed pristine surfaces (accounting for both complementary faces) according to increasing surface energy is (101) < (102) < (112) < [(100), (111)] < (110) < (001). An experimental study of the surface distribution in quartz powders obtained by comminution suggests the following order of crystal form occurrence:[45] $\{101\} + \{0\bar{1}1\} > \{112\} + \{2\bar{1}2\} > [\{100\}, \{001\}, \{2\bar{1}\bar{1}\} + \{111\}] > \{2\bar{1}0\} + \{110\} > \{102\} + \{012\}$. Thus, cleavage probabilities do not correlate well with relaxed surface energies and correlate best with energies of unrelaxed surfaces, as shown elsewhere.[20]

Electronic Structure of Pristine Silica Surface Sites. Electron localization functions (ELF)[46] can be used to describe bonding and location of lone pairs, which can act as sites for electrophilic attack in silica polymorphs.[47] In this work we analyze ELF's of the (110) system in order to gain insights into the electronic structure of relaxed silanone, siloxy, and silyl sites. The ELF value is close to 0.5 in the region where the Pauli repulsion corresponds to that of a homogeneous electron gas, and it is close to 1.0 in the region where the Pauli repulsion is weak (electron pairs or lone electrons).[48] In bulk quartz, bifurcation at ELF = 0.83 divides valence localization domains into monosynaptic V(O) basins and disynaptic valence V(Si,O) basins. The bonding attractors are shifted toward more electronegative oxygen atoms, indicating the partial ionic character of Si−O bonding. Two lone pairs of dicoordinated oxygen atoms of bulk quartz are contained in a single banana-shaped V(O) superbasin. Investigation of ELF and electronic densities obtained in spin-paired DFT calculations shows that silicon atoms of all relaxed sites do not have lone pairs or lone electrons (Figure 2a). Bonding between the silicon atom and unicoordinated oxygen atom of silanone and siloxy sites is partially ionic, with back-donation of lone-pair electrons from unicoordinated oxygen to the valence orbitals of the silicon atom. As a result, a common valence domain around silanone oxygen atom shows two bulges, which are directed toward the silicon atom at ELF = 0.80. This domain bifurcates at ELF = 0.82 into a toroid-shaped V(Si,O) valence disynaptic basin around a line connecting oxygen and silicon atom centers and a bowl-shaped V(O) valence monosynaptic basin. Reconstruction of this surface in spin-polarized calculations with $N_\alpha - N_\beta = 2$ yielded radical siloxy and silyl sites. Silicon atoms of silyl sites have unpaired electron density directed away from the surface (only α-spin monosynaptic valence V(Si) basins are present), while oxygen atoms of siloxy sites exhibit unpaired lone electrons occupying distinct orbitals with one of the spin-electron densities participating more effectively in the bonding between the siloxy silicon atom and siloxy oxygen atom. The ELF pattern of the α-spin density calculations (Figure 2b) shows unpaired electron density around the silyl radical site with a high value of the attractor of ELF = 0.99. In contrast, the ELF pattern of the β-spin density calculations (Figure 2c) reveals a toroid-shaped common valence domain around the siloxy oxygen atom bulged toward silicon atom due to a bonding attractor. It bifurcates into a disynaptic valence basin V(Si,O) and a monosynaptic valence superbasin V(O) encompassing oxygen lone pairs at ELF = 0.80. The latter bifurcates further into two monosynaptic valence V(O) basins at ELF = 0.88.

Silicon−oxygen bonding in two-membered silicon rings, R^2, is weakened compared to the bonding in bulk quartz. Thus, attractors for disynaptic valence V(Si,O) basins have a lower value of ELF = 0.85 in R^2 sites in the $(100)^S$ system compared to ELF = 0.86 in bulk quartz. Lone pairs of electrons on oxygen atoms are less delocalized in R^2 sites, as indicated by a higher value of attractors for monosynaptic valence V(O) basins of ELF = 0.90 vs. ELF = 0.87 in bulk quartz.

A valence V(O) basin of the tricoordinated oxygen atom in the $R_2^2(+)$ site bulges at ELF = 0.84 toward a silicon atom located 1.997 Å from the oxygen. This suggests a donor−acceptor type bonding with electron density of oxygen lone pairs delocalized to vacant orbitals of the silicon atom. Two bonds between this oxygen atom and the other silicon atoms are highlighted by V(Si,O) valence disynaptic basins characteristic of bulk siloxane bonding.

Geometry of Hydrolyzed Quartz Surfaces. Exposure of fractured silica surface to water vapors with partial pressure higher than 1.33 × 10^{-7} Pa results in the hydrolysis of surface sites with the formation of silanol groups, which is completed within 1 h.[49] Hydrolysis of silica surface sites can lead to silanediol ($Q^2(OH)_2$—two geminal silanols), silanetriol ($Q^1(OH)_3$—three geminal silanols), and single silanol (Q^3(OH)) groups. Surface $Q^1(OH)_3$ sites have a low thermal stability[50] and have not been found in NMR studies of natural silicas; hence, further discussion will include only silanediol and single silanol groups.

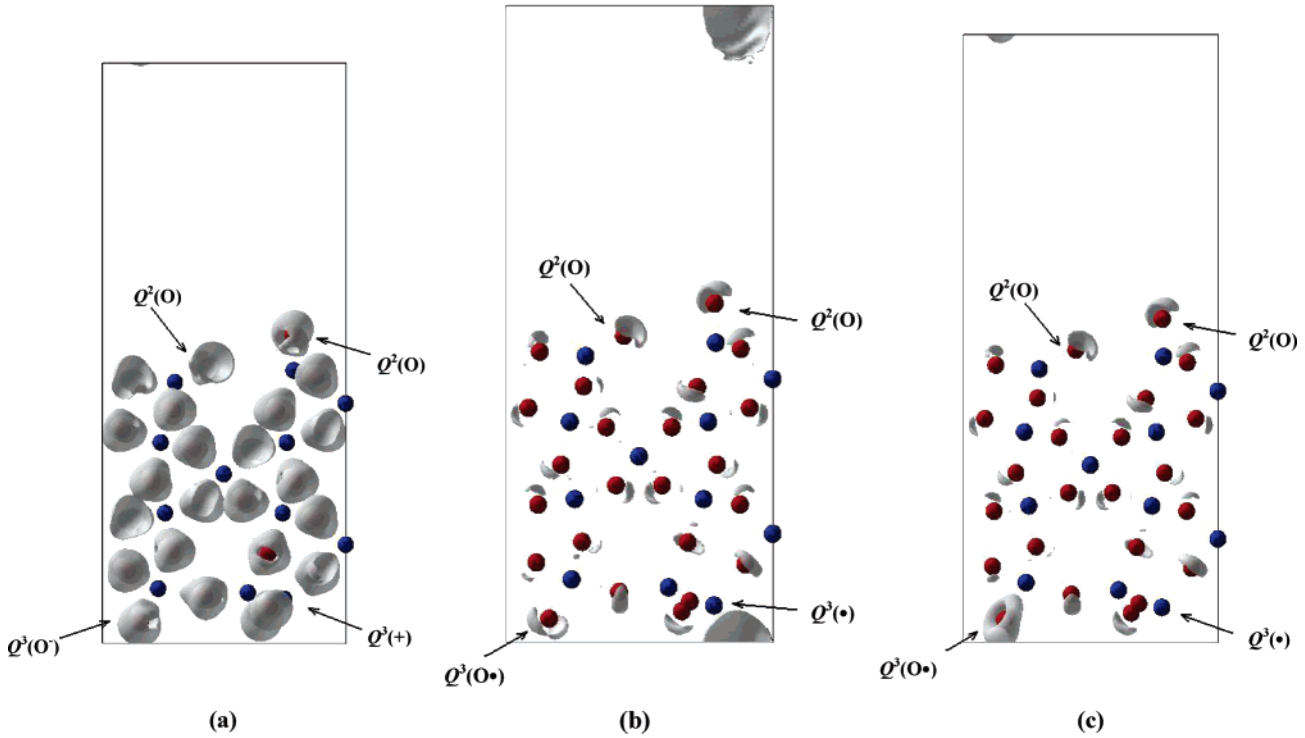

Figure 2. Side projection of reconstructed slabs with pristine (110) complementary surfaces. Iso-ELF surfaces are shown in gray: obtained in spin-paired calculations with ELF = 0.80 (a) and in spin-polarized calculations with $N_\alpha - N_\beta = 2$ and ELF = 0.70 for α-spin density (b) and β-spin density (c).

Propagating zigzag chains of hydrogen-bonded silanol hydroxyls (hydrogen-bond networks) are found on both sides of the (001) slab (parts a and b of Figure 3, r_{Hb} = 1.723 and 2.458 Å on side U and r_{Hb} = 1.737 and 2.424 Å on side D), on silanediol side U of the (110) slab (r_{Hb} = 2.174 and 2.472 Å), on both sides of the (102) slab (the hydrogen bond length sequence is 1.919, 2.225, 3.027, 2.403 Å on side U and 1.866, 2.343, 3.259, 2.369 Å on side D), on side U of the (111) slab (hydrogen bond length sequence is 1.827, 3.035, 2.144 Å), and on the single silanol side U of the (100) slab (r_{Hb} = 1.742 and 2.477 Å). Side D of the (110) slab has inter-silanol hydrogen-bond triplets arranged according to the sequence 1.773, 2.455, 1.784 Å, while side D of the (111) slab has inter-silanol hydrogen-bond doublets with hydrogen bond lengths of 1.842 and 2.177 Å. Isolated inter-silanol hydrogen bonds are found on silanediol side U of the (110) slab (r_{Hb} = 2.079 Å), on silanediol side D of the (100) slab (r_{Hb} = 2.365 Å), and on both sides of the (112) slab (r_{Hb} = 2.852 and 2.942 Å on side U and r_{Hb} = 2.976 and 2.990 Å on side D). There are no inter-silanol hydrogen bonds on the (101) surface. The hydroxyl of a silanol group nearer to the (101) surface is almost parallel to the surface (∠HOsurf = 9°)[51] and points toward the nearest siloxane bridge oxygens with the shortest H···O distances of 2.901 Å. The other hydroxyl points away from the surface with ∠HOsurf = 43°. A geminal silanol, not participating in inter-silanol hydrogen bonding on side D of the (111) slab, points toward siloxane oxygen atoms with the shortest H···O distances of 2.821 Å. As a result, the silanol dips into the surface with ∠HOsurf = −33°. On the (112) surface the shortest H···O distances between silanol hydrogen atoms and siloxane oxygen atoms are 2.784 Å (∠HOsurf = 27°) and 2.834 Å (∠HOsurf = −29°) for sides U and D, respectively.

Relaxation of hydrolyzed quartz surfaces is much less severe compared to reconstruction of pristine surfaces, which is indicated by much lower displacements of the surface atoms (Table 4). This can be explained by the lack of Si−O bond formation or breaking on hydrolyzed silica surfaces. Silicon and oxygen atoms of donor silanol groups participating in short hydrogen bonds and/or of geminal silanol groups undergo the largest displacements. The largest displacement of a silicon atom of 0.154 Å is found for a silanediol site on side U of the (111) surface. The largest displacement of an oxygen atom of 0.485 Å is found for a silanediol site on side U of the (110) surface. On the (001) surface, silicon surface atoms move by 0.04 Å, mostly in the plane of the surface. Oxygen atoms of silanol hydroxyls move by a total of 0.25 Å. An oxygen atom more distant from the surface shifts toward the surface by 0.13 Å, and an oxygen atom nearer to the surface moves away from the surface by 0.13 Å, so that these atoms become located at the same distance from the surface (difference along the normal to the surface is less than 0.002 Å). Slight displacements of silanol oxygen atoms toward silicon atoms on the (101) surface found in this work (ranging between 0.001 and 0.041 Å) are in agreement with experimental X-ray reflectivity studies.[22] On the other hand, on the (100) surfaces half of the single silanol groups move toward silicon atoms by 0.036, while experimental studies indicated an increase of the distance by 0.13 ± 0.04 Å. Oxygen atoms of the other half of silanol groups shift similarly in both studies; i.e. the calculated increase of 0.019 Å falls within experimental error.

Energy of Hydrolyzed Quartz Surfaces. Energies of hydrolyzed surfaces are listed in Table 3. According to our calculations, energy of surface site hydrolysis ranges from −239 kJ/mol for R^2 sites on the (101) surface to −342 kJ/mol for a set of sites on the (112) surface. The order of decreasing stability of hydrolyzed surfaces is (001) > (110) > (102) > (111) > (100) > (112) > (101). This order can be reflected in the frequency of occurrence of crystal faces obtained by mechanical comminution in the presence of water vapors. Surface energy of hydrolyzed quartz surfaces depends on the concentration and strength of hydrogen bonds between vicinal silanol groups. Thus, a transition from exothermic to endothermic heat effects of

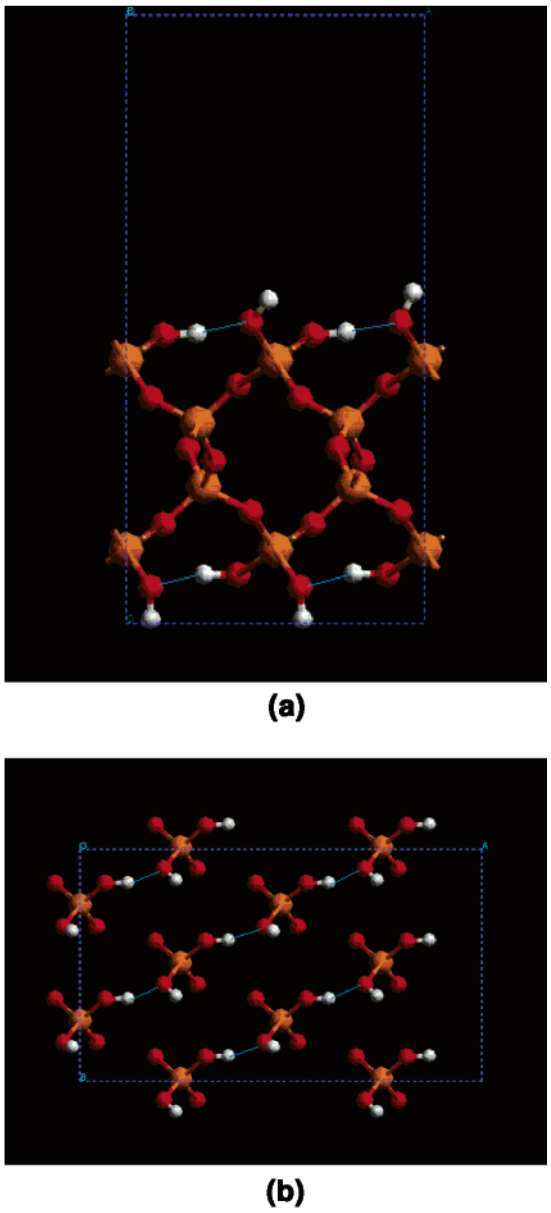

Figure 3. Side (a) and normal (b) projections of a reconstructed slab with hydrolyzed (001) complementary surfaces. Atoms of surface sites are shown as spheres: red for oxygen, white for hydrogen, and orange for silicon. Hydrogen bonds are indicated by blue lines.

hydrolyzed surface formation is observed. The (101) and (112) surfaces with low concentration of single silanol hydroxyls, which are not hydrogen-bonded, require energy for surface formation, while all other surfaces, which have silanediol hydroxyls and intersite hydrogen bonds, release energy (Table 3). Formation of the (001) surface is the most exothermic reaction due to a high concentration of hydrogen-bonded silanol hydroxyls additionally stabilized by the cooperative effect within the hydrogen bond network.[52] Exothermic hydrolysis of siloxane bridges was also reported in earlier calculations[53] on slabs mimicking the (001) surface of β-cristobalite, which contains zigzag chains of hydrogen-bonded silanediol hydroxyls.

No difference in surface energy between geminal silanediol and single silanol groups with the same concentration of silanol hydroxyls was found, once the energy of hydrogen bonds was removed.[54] This becomes transparent after comparing surface energies of a set of (100) face cuts (Table 3). The hydrolyzed (100) surface with only single silanol sites, $(100)^S$, is stabilized by short intersite hydrogen bonds, as indicated by the surface energy of 0.001 eV/Å^2 after the energy of the hydrogen bonds is subtracted (Table 3), which is similar to the surface energy of the hydrolyzed (100) surface with only silanediol sites, $(100)^G$, without short hydrogen bonds. After the energy of hydrogen bonds is removed, the (001) surface shifts from being the most stable to the least stable, while the order of the other faces remains unchanged.

In an aqueous environment, intersite hydrogen-bonded silanol groups are less effective in forming hydrogen bonds with water molecules compared to free-standing silanols. Therefore, additional stabilization due to intersite hydrogen bonds can be negated in aqueous solutions. Intersite silanol hydrogen bonding can also compete with hydrogen bonding to biomolecules and therefore can affect their adsorption.

Conclusions

Four types of reconstruction reactions on pristine low-index quartz surfaces are found. First, this study shows that bridged siloxy and silyl sites reconstruct with the formation of two-membered silicon rings according to the $Q^3(O^-) + Q^3(+) \rightarrow R^2$ reaction on all surfaces investigated. They are stable at ambient temperatures, and their formation requires temperatures higher than 300 K. Second, formation of a $R_2^2(+)$ structure with two side-sharing two-membered rings on the (112) surface is observed in the $R^2 + Q^3(O^-) + Q^3(+) \rightarrow R_2^2(+) + Q^3(O^-)$ reaction. Two geminal oxygen atoms of this structure show a charge alternation: viz., the tricoordinated oxygen atom of the $R_2^2(+)$ structure carries a formal positive charge of +1, while the unicoordinated siloxy oxygen atom has a formal negative charge of −1. Third, the reconstruction $Q^4 + Q^3(O^-) \rightarrow Q^3(O^-) + Q^4$ around a $Q^3(+)$ silyl site, resulting in the formation of a three-membered silicon ring, R^3, is also found on the (112) surface. Fourth, the reconstruction $Q^2(O) + Q^3(+/\bullet) \rightarrow Q^4 + Q^3(+/\bullet)$ reaction on the (110) surface involves a siloxane-bridge relocation and a siloxane-bridge formation. It also leads to the formation of a four-membered silicon ring, R^4. In agreement with experimental study, only a (1 × 1) pattern is found on the pristine (001) surface covered with relaxed silanone sites. Geometries of silica sites obtained in these periodic calculations correlate well with those found in cluster calculations. Surfaces with charged siloxy anion and silyl cation sites (heterolytic cleavage) are found to be more stable energetically by 104 kJ per mole of silyl and siloxy sites as compared to surfaces with radical siloxy and silyl sites (homolytic cleavage). This is explained by favorable intersite electrostatic interactions between charged sites. The order of reconstructed pristine surfaces according to increasing surface energy is (101) < (102) < (112) < [(100), (111)] < (110) < (001).

Hydrolyzed surfaces are stabilized by hydrogen bonds between vicinal silanol groups. Vicinal geminal groups almost always form intersite hydrogen bonds, while vicinal single silanol groups are bonded only on the (100) surface. Networks of hydrogen bonds are found on all surfaces, except for the (112) and (101) surfaces with only single silanol groups. The magnitude of relaxation of hydrolyzed silica surfaces is much lower compared to reconstruction of pristine silica surfaces. The order of decreasing stability of hydrolyzed surfaces is (001) > (110) > (102) > (111) > (100) > (112) > (101). This order could be reflected in the frequency of occurrence of crystal faces obtained by mechanical comminution in the presence of water vapors. Subtraction of hydrogen-bond energy increases the surface energy of the (001) surface from the lowest to the highest.

Analysis of surface energies of (100) quartz surfaces covered with either geminal silanediol or single silanol sites suggests

that crystalline silica surfaces with geminal silanediol groups can be readily formed in mechanical comminution processes in vacuo, while those with single silanol groups can be dominant on crystals naturally grown from melts and solutions or on crystals, which underwent an extensive long-term reconstruction or refaceting.

Information about pristine and hydrolyzed quartz surface relaxation obtained in this work could be further utilized in computer modeling of interactions between silica surfaces and biological macromolecules in order to gain insights into the nature of silicosis.

References and Notes

(1) NIOSH Hazard Review: Health Effects of Occupational Exposure to Respirable Crystalline Silica. DHHS (NIOSH) Publication No. 2002−129.

(2) Nash, T.; Alison, A. C.; Harington, J. S. *Nature* **1966**, *211*, 259.

(3) Murashov, V. V.; Demchuk, E.; Harper, M. To be submitted for publication.

(4) Radtsig, V. A. *Kinet. Catal*. **1999**, *40*, 693.

(5) Hochstrasser, G.; Antonini, J. F. *Surf. Sci*. **1972**, *32*, 644.

(6) Raghavachari, K.; Pacchioni, G. *J. Chem. Phys*. **2001**, *114*, 4657.

(7) Zyubin, A. S.; Mebel, A. M.; Lin, S. H.; Glinka, Y. D. *J. Chem. Phys*. **2002**, *116*, 9889.

(8) Radtsig, V. A.; Berestetskaya, I. V.; Kostritsa, S. N. *Kinet. Catal*. **1998**, *6*, 863.

(9) Morrow, B. A.; Cody, I. A. *J. Phys. Chem*. **1976**, *80*, 1995.

(10) Michalske, T. A.; Bunker, B. C. *J. Appl. Phys*. **1984**, *56*, 2686.

(11) Burneau, A.; Barres, O.; Gallas, J. P.; Lavalley, J. C. *Langmuir* **1990**, *6*, 1364.

(12) Maciel, G. E.; Sindorf, D. W. *J. Am. Chem. Soc*. **1980**, *102*, 7606.

(13) Okada, K.; Kameshima, Y.; Yasumori, A. *J. Am. Ceram. Soc*. **1998**, *81*, 1970.

(14) Duval, Y.; Mielczarski, J. A.; Pokrovsky, O. S.; Mielczarski, E.; Ehrhardt, J. J. *J. Phys. Chem. B* **2002**, *106*, 2937.

(15) Murashov, V. V. *J. Mol. Struct*. **2003**, *650*, 141.

(16) In this work reconstruction means changes in bonding pattern and relaxation means changes in bond lengths and bond angles.

(17) Bart, F.; Gautier, M. *Surf. Sci. Lett*. **1994**, *311*, L671.

(18) Janossy, I.; Menyhard, M. *Surf. Sci*. **1971**, *25*, 647.

(19) Rignanese, G.-M.; De Vita, A.; Charlier, J.-C.; Gonze, X.; Car, R. *Phys. Rev. B* **2000**, *61*, 13250.

(20) Murashov, V. V.; Demchuk, E. To be submitted for publication.

(21) In this paper the NMR classification is adopted to describe surface sites. Thus, Q^n represents a silicon atom under consideration with n attached silica units. Surface termination of Q units by X species follows the description of a surface site. For example, a surface geminal silanediol site, X = OH, can be categorized as $Q^2(OH)_2$.

(22) Schlegel, M. L.; Nagy, K. L.; Fenter, P.; Sturchio, N. C. *Geochim. Cosmochim. Acta* **2002**, *66*, 3037.

(23) Konecny, R.; Leonard, S.; Shi, X.; Robinson, V.; Castranova, V. *J. Environ. Path. Tox. Oncol.* **2001**, *20* (Suppl. 1), 119.

(24) de Leeuw, N. H.; Higgins, F. M.; Parker, S. C. *J. Phys. Chem. B* **1999**, *103*, 1270.

(25) Baram, P. S.; Parker, S. C. *Philos. Mag. B* **1996**, *73*, 49.

(26) Kresse, G.; Hafner, J. *Phys. Rev. B* **1993**, *48*, 13115. Kresse, G.; Hafner, J. *Phys. Rev. B* **1994**, *49*, 14251.

(27) Kresse, G.; Furthmüller, J. *Comput. Mater. Sci*. **1996**, 6, 15. Kresse, G.; Furthmüller, J. *Phys. Rev. B* **1996**, *54*, 11169.

(28) Perdew, J. P.; Chevary, J. A.; Vosko, S. H.; Jackson, K. A.; Pedersen, M. R.; Singh, D. J.; Fiolhais, C. *Phys. Rev. B* **1992**, *46*, 6671.

(29) Kresse, G.; Joubert, D. *Phys. Rev. B* **1999**, *59*, 1758.

(30) Vanderbilt, D. *Phys. Rev. B* **1990**, *41*, 7892.

(31) Kresse, G.; Hafner, J. *J. Phys.: Condens. Matter* **1994**, *6*, 8245.

(32) Monkhorst, H. J.; Pack, J. D. *Phys. Rev. B* **1976**, *13*, 5188.

(33) Jepsen, O.; Andersen, O. K. *Solid State Commun*. **1991**, *9*, 1763.

(34) Blöchl, P.; Jepsen, O.; Andersen, O. K. *Phys. Rev. B* **1994**, *49*, 16223.

(35) α-Quartz belongs to the trigonal trapezohedral class of the hexagonal system; the optically/morphologically right-handed and structurally left-handed enantiomorph has $P3_221$ space group symmetry.

(36) Wyckoff, R. W. G. *Crystal Structures*; Wiley: New York, 1960; Vol. 4.

(37) Experimental values are given in parentheses.

(38) Convergence of slab energy on interslab separation for the (001) surface was tested, and an increase of up to 20 Å was found to result in a change of the total slab energy of 3.5×10^{-4} eV or (3×10^{-4})% only.

(39) Curtiss, L. A.; Frurip, D. J.; Blander, M. *J. Chem. Phys*. **1979**, *71*, 2703.

(40) Levine, S. M.; Garofalini, S. H. In *Defects in Glasses*, Proc. Mater. Research Soc. Symp. 61; Galeener, F. L., Griscom, D. L., Weber, M. J., Eds.; Materials Research Society, Pittsburgh, PA, 1985; pp 28−37.

(41) Ceresoli, D.; Bernasconi, M.; Iarlori, S.; Parrinello, M.; Tosatti, E. *Phys. Rev. Lett*. **2000**, *84*, 3887.

(42) Planarity of a $Q^3(+/\bullet)$ site is characterized by a torsion angle between two Si−O bonds around the third Si−O bond. Thus, a perfectly planar site is described by OSiOO torsion angles of 180°.

(43) Gibbs, J. W. *Collected Works*; Longman: New York, 1928.

(44) Lucovsky, G. J. *Non-Cryst. Solids* **1980**, *35/36*, 825.

(45) Bloss, F. B.; Gibbs, G. V. *Am. Miner*. **1963**, *48*, 821.

(46) In this work VaspView software (http://vaspview.sourceforge.net/) was used to visualize ELF functions.

(47) Gibbs, G. V.; Cox, D. F.; Crawford, T. D.; Boisen, M. B.; Lim, M. *Phys. Chem. Miner*. **2002**, *29*, 307.

(48) Savin, A.; Nesper, R.; Wengert, S.; Fassler, T. F. *Angew. Chem., Int. Ed. Engl.* **1997**, *36*, 1809.

(49) D'Souza, A. S.; Pantano, C. G. *J. Am. Ceram. Soc*. **1999**, *82*, 1289.

(50) Severin, J. W.; Vankan, J. M. J. *Philips J. Res*. **1990**, *45*, 35.

(51) An angle between a silanol hydroxyl bond and a surface.

(52) Frank, H. S.; Wen, W.-Y. *Discuss. Faraday Soc*. **1957**, *24*, 133. Del Bene, J.; Pople, J. A. *Chem. Phys. Lett*. **1969**, *4*, 426.

(53) Vigné-Maeder, F.; Sautet, P. *J. Phys. Chem. B* **1997**, *101*, 8197.

(54) It is assumed that the energy of a single intersite hydrogen bond shorter than 2.00 Å is equal to the energy of the hydrogen bond in the water dimer. This approach to the calculation of "hydrogen-bond-free" surface energies $E_{surf-Hb}$ provides a very rough estimate only, and its results should be used with caution.